

## Characterization of Self-assembled Electrodes Based on Au-Pt Nanoparticles for PEMFC Application

E. Valenzuela<sup>1</sup>, P.J. Sebastian<sup>2,\*</sup>, S.A. Gamboa<sup>2</sup>, Shine Joseph<sup>2</sup>, and U. Pal<sup>3</sup>, I. Gonzalez<sup>4</sup>

<sup>1</sup>Energía y Sustentabilidad, Universidad Politécnica de Chiapas, Tuxtla Gutiérrez, Chiapas, México

<sup>2</sup>Centro de Investigación en Energía, Universidad Nacional Autónoma de México, Temixco 62580, Morelos, México

<sup>3</sup>Instituto de Física, Universidad Autónoma de Puebla, Puebla, Pue. 72570, México.

<sup>4</sup>Universidad Autónoma Metropolitana, Departamento de Química, 09340, México.

Received: July 29, 2009, Accepted: August 4, 2009

**Abstract:** In this article we report the synthesis and characterization of Au, Pt and Au-Pt nanoparticles impregnated on Nafion membrane for the proton exchange membrane fuel cell (PEMFC) application. Colloidal solutions were used to prepare self-assembled electrodes with nanoparticles deposited on Nafion membrane. The particles deposited on Nafion had good stability and homogeneous distribution along the membrane surface. The impedance results proved an increase in the membrane proton resistance of the self-assembled electrodes compared to unmodified Nafion. The increase in resistance is related to the diminution of the protonic charge carriers in the Nafion nano-channels near the surface due to the channel obstruction by the deposited particles.

**Keywords:** PEM fuel cell, Nafion, Au-Pt, Nanoparticles, Protonic conduction.

### 1. INTRODUCTION

Proton Exchange Membrane Fuel Cells (PEMFC) are highly efficient devices for electrical power generation. Besides the high efficiency, PEMFC has no moving parts and when pure hydrogen is used as fuel the only by-product is water [1, 2]. The PEMFC has high energy density (higher than 1 kW/L), quick start up and low operating temperature (80–100°C) [3,4]. These properties make PEMFC adequate for powering mobile devices such as cell phones, personal computers and as a power source in automotive applications.

Despite the advantages of the PEMFC system, its application is still limited because of the cost of manufacturing materials, mainly the electrolyte and the electrocatalysts. Actually the mostly used catalyst is Pt, a very expensive material that has made difficult the massive commercialization of PEMFC.

Since the research on PEMFC started, the loading of Pt has decreased from 1 g/cm<sup>2</sup> up to 0.4 mg/cm<sup>2</sup> or less without sacrificing the performance and reliability [5,6]. The diminution in Pt loading has made possible by increasing both the catalyst area and the

reaction sites in the electrodes. One of the best options for improving the catalyst efficiency is by using nanostructured materials. The considerably higher area of nanoparticle catalyst compared to microcrystalline metallic particles, and the changes in the material properties due quantum confinement increase the reaction rates, efficiency and allow substituting actual catalyst materials [7-9].

Another improvement that would reduce the cost of PEMFC is the simplification of the manufacturing process, especially, the Membrane-Electrode Assemble (MEA). Several attempts have been made to simplify this process. The objective of this study is to develop a simple and low cost method to optimize the catalyst performance. Normally, the MEA is made by diluting Pt/C and Nafion in isopropanol, after that the ink is applied on the membrane by painting, spraying or printing. Finally the gas diffusers are attached by hot pressing [7]. The disadvantage of these methods is the low Pt utilization, since only 10% of Pt is located in active sites where the chemical reaction takes place [8,9]. Despite one of the best options for the efficient use of Pt in MEA fabrication is the sputtering technique [10], fabricating the MEA by the sputtering technique is expensive and complicated, so it is necessary to continue investigating for new options that compromise efficiency, cost and simplicity.

\*To whom correspondence should be addressed: Email: sjp@cie.unam.mx,  
Phone: +52 55 56229841, Fax +52 55 56229742

### 1.1. Au and AuPt alloys as catalysts in PEMFC

Historically Au has been considered as a stable material with low catalytic activity [11], however the results obtained by Haruta [12] and Hutchings [13] showed that Au nanoparticles exhibit good superficial reactivity. Actually it is known that when well prepared, Au is an excellent and a CO tolerant electrocatalyst in several electrochemical processes [11,14,15]. Electrocatalysts with lower cost, CO tolerance and high performance, are the best suited materials for PEMFC electrodes. Recent results show that nanostructured Au and AuPt catalysts (2-5 nm and Au>70%) have a similar or better performance than Pt/C and PtRu/C in the oxygen reduction reaction (ORR) with only 10-25% of the metal content [16-18].

The aim of this work is to fabricate MEAs by depositing Au, Pt and AuPt nanoparticles on Nafion 115 by immersion, a method for simplifying the electrode fabrication. The nanoparticle catalyst activity was measured with Rotating Disc Electrode (RDE). After deposition of the nanoparticles on the membrane, the surface was studied by Scanning Electron Microscopy (SEM) and Energy Dispersive Spectroscopy (EDS); the membrane proton conduction process was studied by Electrochemical Impedance Spectroscopy (EIS) with the four probe technique, finally the MEAs fabricated with Nafion/Metal membranes were evaluated in a PEMFC under standard conditions.

## 2. EXPERIMENTAL DETAILS

### 2.1. Nanoparticle Synthesis

The Au, Pt and AuPt nanoparticles were synthesized by chemical reduction of  $\text{HAuCl}_4$  and  $\text{H}_2\text{PtCl}_6$  with  $\text{NaBH}_4$ , in a solution of polyvinyl pyrrolidone (PVP) and methanol as a protective agent. The protective agent was obtained dissolving 150 mg of PVP in 50 ml of methanol. A solution of 0.56 mg of  $\text{HAuCl}_4$  in 50 ml of de-ionized water was used as a precursor for the Au nanoparticles. The Au nanoparticles were obtained by mixing the protective agent and the precursor, followed by adding a reducing solution of 14.96 mg of  $\text{NaBH}_4$  in 6 ml of water. The reaction mixture was stirred for 15 minutes at 25°C. The same procedure was applied for the Pt nanoparticle synthesis; 50 ml of protective agent was mixed with a solution of 1.23 mg of  $\text{H}_2\text{PtCl}_6$  in 50 ml of de-ionized water, 14.96 mg of  $\text{NaBH}_4$  in 6 ml of water was added to the mixture and then stirred for 15 min at 25°C. The bimetallic AuPt [1:1] nanoparticles were obtained by simultaneous chemical reduction of Au and Pt ions. 0.56mg of  $\text{HAuCl}_4$  and 1.23 mg of  $\text{H}_2\text{PtCl}_6$  were dissolved in 100 ml of de-ionized water. The precursors were reduced by adding a solution of 29.93 mg of  $\text{NaBH}_4$  in 12 ml of water. The mixture was stirred for 15 min at 25°C. While adding the reducing agent, the solution changed color from yellow to brown for Pt and AuPt nanoparticles and from yellow to red for Au colloids.

### 2.2. RDE (Rotating Disc Electrode)

The nanoparticles were supported on carbon black (Vulcan XC72) by the following procedure; 2 mg of carbon black was oxidized with 1 ml of  $\text{H}_2\text{O}_2$  (30%) at 40°C. Before the sample was dried, 1 ml of colloidal dispersion was added, and then treated at 330°C in nitrogen for 20 minutes. The catalytic ink was prepared with 10 ml of Nafion and the nanoparticles were supported on carbon. The mixture was diluted in isopropanol and mixed in an ultrasonic agitator for 20 min. After that, 5 ml of this solution was placed in the rotating disc electrode and let to dry at 25°C.

The catalytic properties of Au-Pt were evaluated by linear voltamperometry with the RDE technique in a 3 electrode cell. The electrochemical tests were performed using a Pt grid as counterelectrode and a  $\text{Hg}/\text{Hg}_2\text{SO}_4$  as the reference electrode. The tests were made in 0.5 M  $\text{H}_2\text{SO}_4$  as electrolyte at ambient temperature under saturated oxygen conditions. The results were recorded with a Solartron SI 1287 Potentionstat/Galvanostat. The open circuit potential was measured and the test started when a variation lower than 5 mV/min was observed. The linear voltamperometry was recorded from -0.6 to 0.3 V at 10 mV/s, changing the rotation speed from 100 to 1800 rpm in steps of 100 rpm.

### 2.3. Membrane Activation and Impregnation

The membranes were first purified in 3 %  $\text{H}_2\text{O}_2$  at 80°C for 30 min, and then rinsed twice in de-ionized water at 100°C for 30 min. The membranes were then protonated in 1 M  $\text{H}_2\text{SO}_4$  at 85°C. The membranes were kept 48 hrs in  $\text{H}_2\text{SO}_4$  at ambient temperature to ensure adequate protonation. After that, the membranes were rinsed twice in boiling water for 30 min and then stored in de-ionized water. After the membrane protonation the Au-Pt nanoparticles were deposited on Nafion 115 by immersion, the membranes were completely immersed in colloidal dispersions for 1 hr and then rinsed with de-ionized water. The membrane color changed to brown for Pt and AuPt and purple for Au colloids. A total of three membranes were impregnated, Au, Pt and AuPt [1:1].

### 2.4. SEM (Scanning Electron Microscopy)

For the superficial study on Nafion and Nafion/Au-Pt, four samples were activated and impregnated, Nafion-Au, Nafion-Pt, Nafion-AuPt and Nafion as reference. Once the nanoparticles were deposited the samples were dried at ambient temperature for 1 hr. The micrographs were obtained in a SEM JEOL-JSM-6400 under 25 kV potential. The Elemental Mapping was obtained with a NO-RAN EDS, a 33 x 33 mm was analyzed in steps of 250 nm, the area was scanned 30 times and then the elemental distribution was plotted.

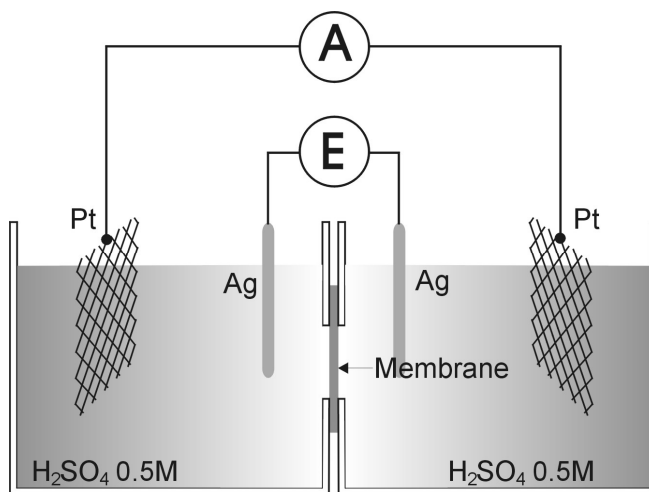


Figure 1. The typical electrochemical cell for EIS in proton conduction membranes, two Pt counter electrodes force a proton current through the membrane and the potential in each side of the membrane is measured, the current and potential values are used to calculate the membrane impedance.

### 2.5 EIS. (Electrochemical Impedance Spectroscopy)

One of the major disadvantages of studying the complete fuel cell impedance response is the complexity to separate the contributions of each component of the cell [19-21]. Based on the limitations of the methods used until now, a new experimental system was designed and built to measure easily and accurately the EIS response of a membrane and a membrane electrode assembly under fuel cell operating conditions. The experimental designs reported [22-24] were modified to obtain a measurement system that provides accurate and easy to obtain information about the membrane proton conduction process by means of electrochemical impedance response.

For the study of the proton conduction process of the Nafion and impregnated membranes a Proton Transfer cell was designed and built. The EIS diagrams were obtained using the four probe technique. The electrochemical cell is shown in figure 1. The membrane was placed in between two half-cells separating the electrolyte of each half-cell; two Pt grids were used as counter electrodes on each side of the membrane. The area of the Pt grids ( $2 \text{ cm}^2$ ) was larger than the area of the membrane to avoid current limitations due to the counter electrodes. Two Ag wires (1 cm long and  $0.78 \text{ mm}^2$  area) were used as pseudo-reference electrodes. The tests were done in  $0.5 \text{ M H}_2\text{SO}_4$  with a Potentiostat/Galvanostat Solartron SI 1287 at  $25^\circ\text{C}$ . The impedance was measured in a frequency range from  $1 \times 10^6$  to 100 Hz. After starting the experiment the Ag wires were let to passivate in  $\text{H}_2\text{SO}_4$  in order to have a stable potential, the open potential between both sides of the membrane was measured and the experiment was started when the open potential was between 0 and 5 mV with a variation smaller than 5 mV/min.

### 2.6. Polarization Curves

The MEAs fabricated with nanoparticles deposited on Nafion 115 were evaluated in a PEMFC. The catalytic ink for the electrodes was prepared diluting 10 % Pt/C ( $0.4 \text{ mg/cm}^2$ ) and 11 ml of Nafion in isopropanol, the ink was applied on the membranes modified with nanoparticles by the painting technique. The carbon cloth diffusers were attached by hot pressing at  $100 \text{ Kg/cm}^2$  and  $140^\circ\text{C}$  for 5 min. The electrical parameters of the fuel cell were evaluated at  $25^\circ\text{C}$  with a flow of  $100 \text{ cc/min}$  of hydrogen in the anode and  $80 \text{ cc/min}$  of oxygen in the cathode. A Scribner Associates 890 Series Load Unit was used to measure the fuel cell electrical parameters. The electrical conversion efficiency at  $200 \text{ mA/cm}^2$  was calculated and the current density vs. power density was plotted to find out the optimal working current.

## 3. RESULTS AND DISCUSSION

### 3.1. TEM (Transmission Electronic Microscopy)

The Au-Pt nanoparticles synthesized by chemical reduction were characterized by Transmission Electronic Microscopy in a Philips Tecnai 200 TEM. A drop of the sample was taken from the surface of the nanoparticle colloidal dispersions and placed on a copper grid. Once the sample was dried, the nanoparticles were studied in the microscope. The samples were analyzed to determine the shape and the mean size of the nanoparticles.

The TEM analysis of the Au-Pt nanoparticles (fig 2) showed a good dispersion of particles with some agglomerations of well identified particles. The particles were close to spherical shape and no formation of nanowires or nanorods was observed. This particle

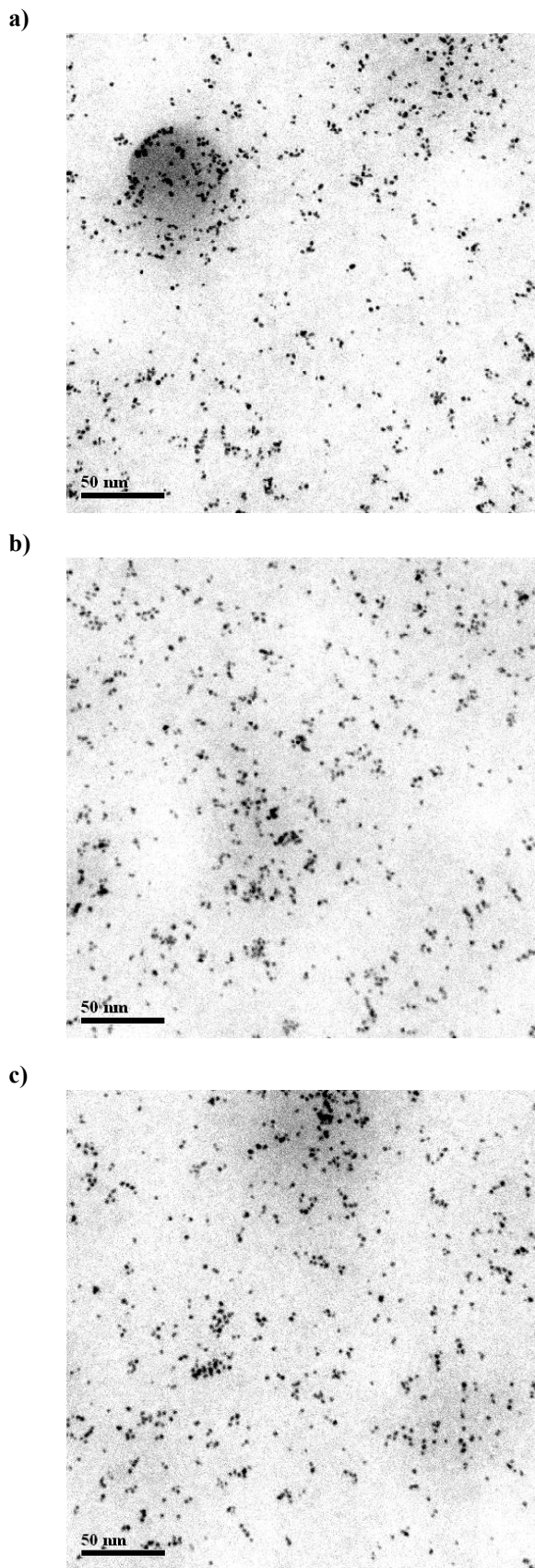


Figure 2. The TEM micrographs for the colloidal nanoparticles, a) Au, b) Pt, c) AuPt.

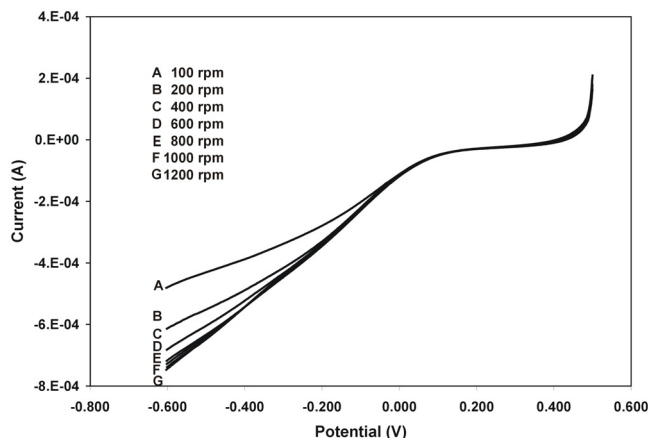


Figure 3. The RDE results for the Au nanoparticles.

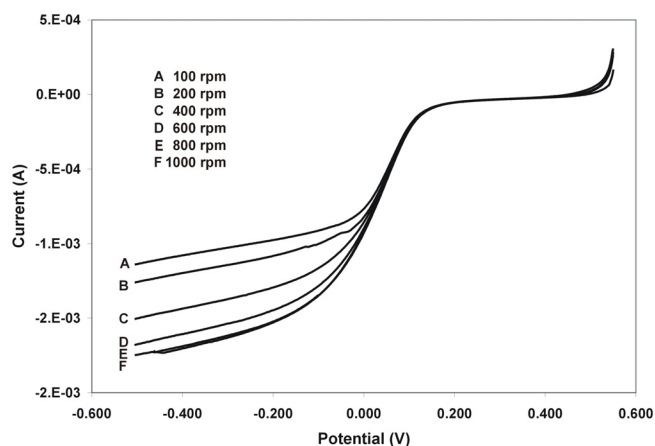


Figure 4. The RDE results for the AuPt nanoparticles.

Table 1. Table 1. Kinetic data from the RDE experiments for the Au, AuPt and Pt nanoparticles.

Material	Tafel Slope	b	na
Au	6.78	0.3396	0.1750
AuPt	10.21	0.2255	0.2636
Pt	13.89	0.1658	0.3585

size and shape is related to the synthesis process and the type of reducing agent. The mean size of the nanoparticles was obtained by a distribution analysis considering more than 100 particles in all the three cases. The particles were counted in the TEM micrographs shown in figure 2. The mean particle size calculated for the Au and Pt nanoparticles was about 2 nm (fig 2.a and 2.b). The size of the AuPt nanoparticle was about 3 nm (fig 2.c). The standard deviation in the three analyses was lower than 0.4 nm. This particle size is among the reported values for Au-Pt nanoparticles obtained by chemical reduction and in accordance with theoretical results. This particle size is in the optimum range for its possible application as electrocatalyst in PEMFC.

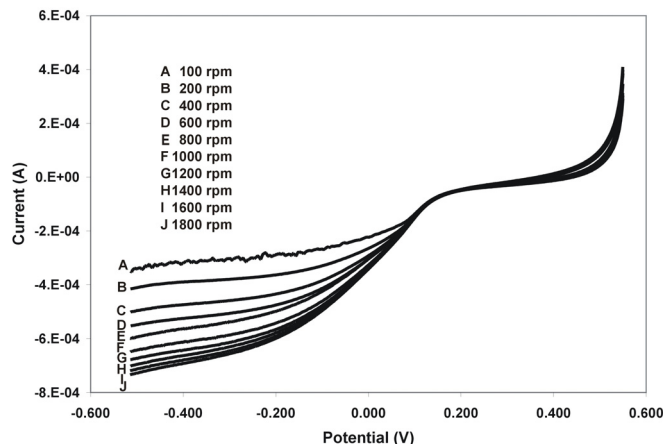


Figure 5. The RDE results for the Pt nanoparticles.

### 3.2. RDE (Rotating Disk Electrode)

The catalytic activity of the Au, Pt and AuPt nanoparticles for the oxygen reduction was studied by linear voltamperometry. The nanoparticles were deposited on carbon and evaluated in a Rotating Disk Electrode under oxygen bubbling in the electrolyte. The open circuit potentials were 153 mV for Au, 197 mV for AuPt and 228 mV for Pt. Figure 3 shows the results obtained for the Au nanoparticles. The nanostructured Au catalyst showed acceptable performance compared to the results already published [25]. In figure 3 one can identify the kinetic threshold at 130 mV (Vs Hg/Hg<sub>2</sub>SO<sub>4</sub>). For rotation speeds higher than 600 rpm there is no change in the limiting current. This result suggests that even when there is flow of new species to the electrode surface, the catalyst is not able to increase the speed of the reaction.

For the AuPt [1:1] nanostructured catalyst (fig 4), the kinetic threshold can be identified at 150 mV (Vs Hg/Hg<sub>2</sub>SO<sub>4</sub>). The limiting current is reached at a lower potential than that for Au catalyst (-500 mV for AuPt, for Au catalyst the limiting current was not reached).

For the nanostructured Pt system, the kinetic threshold was identified at 160 mV (figure 5, vs. Hg/Hg<sub>2</sub>SO<sub>4</sub>). In figure 5 it can be seen that the current reaches a stationary state around -500 mV. The limiting current shows a direct relation with the rotating speed. For this system it was possible to reach the maximum rotating speed of 1800 rpm, which suggests a better catalyst performance than the Au and the AuPt systems.

The results of table 1 show a better catalytic performance for the Pt nanoparticles. The Tafel slope for the Au nanoparticles is lower compared to AuPt and Pt suggesting a lower reaction kinetic compared to AuPt and Pt. Also, the na value and the kinetic threshold voltage suggest a less reductive system for the Au particles than the values calculated for Pt and AuPt.

Once the particle dispersion, size and the catalytic properties were studied, the self-assembled Nafion/Nanoparticles were fabricated using the dip coating method. The superficial and electrochemical studies are shown in the next section.

### 3.3. SEM (Scanning Electron Microscopy)

#### 3.3.1. Nafion

The Nafion and Nafion/Nanoparticle self-assemblies were stu-

died by Scanning Electron Microscopy using backscattered electrons (fig 6). The Nafion membrane shows a typical rough surface with slight changes in contrast due to the hydrophobic and hydrophilic phases randomly distributed in the membrane. The backscattered electron micrographs allow identifying high atomic mass elements such as Au and Pt in the Nafion surface. In all the self-assemblies the Au-Pt particles dispersed in the Nafion surface without the formation of a continuous layer can be seen.

It can be seen in the modified membranes (fig 6b, 6c, 6d) the presence of the metallic particles along the membranes surface. The nanoparticles were accumulated forming structures with different size (up to  $\mu\text{m}$ ) and shape. The size of the deposited particles varies from 10 to 1 nm, and in some cases the particles are so small that its presence was only revealed by an EDS analysis. The distribution and size of the particles over the Nafion corresponds to the relation between the membrane and the nanoparticle of the elements, this phenomenon is explained in the analysis of the Elemental Mapping.

### 3.3.2. Elemental Mapping

An elemental Mapping analysis was performed in order to study the Au and Pt location in the self-assemblies. Figure 7 shows the results of the elemental mapping, the black dots represent the metallic particles (Au and Pt).

The structural properties of the Nafion membrane determine the distribution and particle size deposited on the membrane. Nafion is composed of a hydrophilic phase formed by interconnected groups of micelles randomly distributed over a hydrophobic matrix [26,27]. The maximum particle size of Au-Pt particles deposited on Nafion by chemical reduction is restricted by the hydrophilic cluster size [28,29]. Nevertheless, when methanol is involved in the nanoparticle synthesis, there is evidence of particle formation with an average size bigger than the hydrophilic cluster size. This increase in the particle size on the Nafion is related to the diminution of the hydrophobic properties of the PTFE backbone membrane, which causes the merger of neighboring micelles leading to an increase in the hydrophilic cluster size and consequently to the bigger particle formation [30]. The elemental mapping results prove that the Au and Pt is deposited and dispersed all over the membrane. The results showed an adequate distribution of the material on the Nafion surface, with no evidence of layers of Au-Pt formation.

### 3.3.3. Composition analysis

Based on the EDS analysis the deposit composition was determined with an error lower than 1 At %. The Nafion elements were identified as F, C and S, and in the self-assembled electrodes Au and Pt as evidence of the deposit. The composition analysis showed a similar trend for all the impregnated membranes, even in surface points where apparently there is no particle formation. Table 2 shows the At % of Au and Pt deposited on the membrane, it can be seen that Pt has a better interaction with Nafion and hence, the quantity of Pt deposited is higher than that of Au. In the membrane modified with AuPt nanoparticles, even though the proportion of Au and Pt used in the nanoparticle synthesis was 1:1, the analysis shows a Pt:Au proportion of 3: 1 in the deposit, which confirms the better affinity of Nafion for Pt.

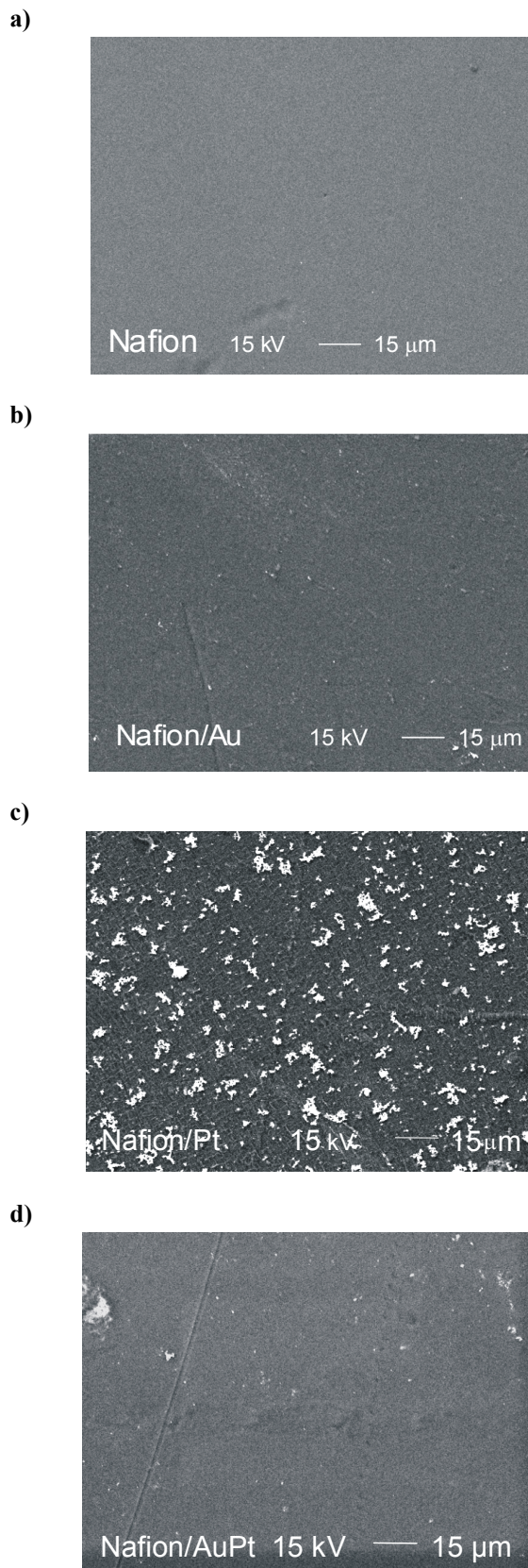


Figure 6. The SEM micrographs showing the Au, AuPt and Pt deposited in the self-assembly.

Table 2. The composition analysis results for Au and Pt in the self-assemblies.

Sample	Atomic %	C	O	F	Pt	Au	S
Nafion		19.83	9.47	65.64	-0-	-0-	5.24
Nafion/Au		28.18	7.38	59.68	-0-	<b>0.56</b>	3.86
Nafion/Pt		25.66	6.44	61.48	<b>3.45</b>	-0-	2.98
Nafion/AuPt		26.94	6.19	62.77	<b>0.98</b>	<b>0.30</b>	2.82

Table 3. The value of the electrical parameters for the elements of each equivalent electrical circuit.

	$R_s (\Omega)$	$R_{HT} (\Omega)$	$R_{DBL} (\Omega)$	$Q_1 (10^{-5})$	$\eta_1$	$Q_2 (10^{-5})$	$\eta_2$
Nafion	50.21	0.0600	0.3600	100.0	0.90	66.03	0.94
Nafion /Pt	50.04	0.1200	0.7700	20.00	1.10	8.49	0.90
Nafion /Au	45.25	0.1611	0.8800	26.00	0.70	4.90	0.90
Nafion /AuPt	69.25	0.2500	0.8400	70.00	1.00	4.16	0.93

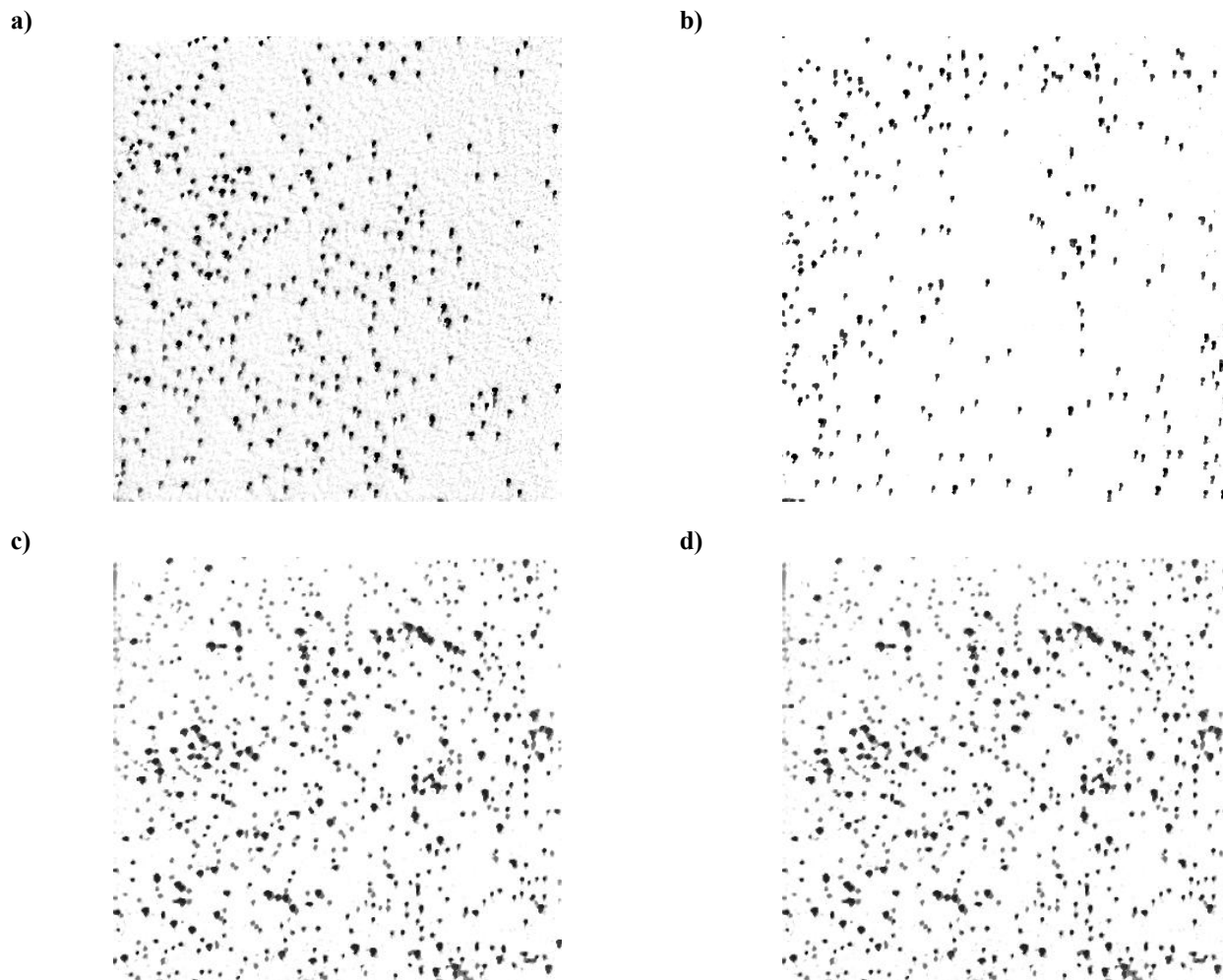


Figure 7. The elemental mapping analysis showing the Au-Pt particle location related to the hydrophilic and hydrophobic distribution in the Nafion membrane.

Table 4. The electrical characteristics obtained for the self-assembled electrodes evaluated in a PEMFC.

	Open circuit potential (mV)	Short circuit current density (mA/cm <sup>2</sup> )	Maximum power density (mW/cm <sup>2</sup> )	Efficiency (%) at 200 mA/cm <sup>2</sup>
Nafion/Au	735	337	68.87	22
Nafion/AuPt	887	446	83.30	26
Nafion/Pt	815	446	83.81	26

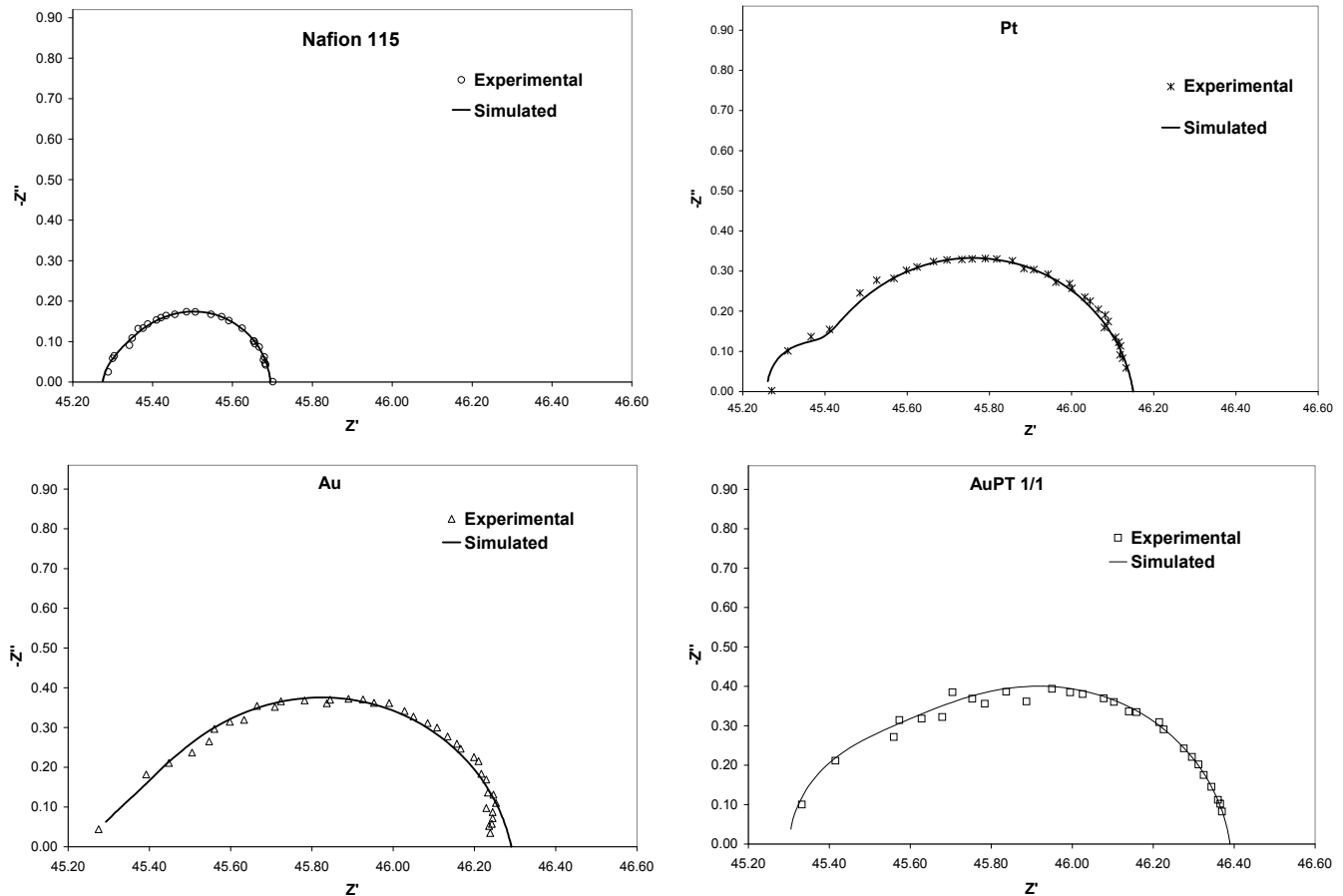


Figure 8. The Nyquist diagrams for the Nafion 115 and the self-assembled electrodes. Both systems show a typical conductive membrane response, two semicircles overlapped at medium frequencies.

### 3.4 Nyquist Diagrams

#### 3.4.1. EIS

The self-assembled electrodes were studied by electrochemical impedance in a 4 electrode cell. The Nyquist plots are shown in figure 8. In the Nyquist diagrams for Nafion and impregnated Nafion, it can be seen that all the plots correspond to a typical membrane electrolyte system, two semicircles overlapped at medium frequencies (1 kHz). The Nyquist diagrams were well adjusted with the Z-View 2.8 software and hence using the electrical equivalent circuit for conducting membrane systems (fig 9). Table 3 shows the values of the electrical circuit elements for each membrane. In all the systems the value of the resistance of the low frequency process is higher than the resistance in the high frequency process, which suggests that the protonic charge transference in the membra-

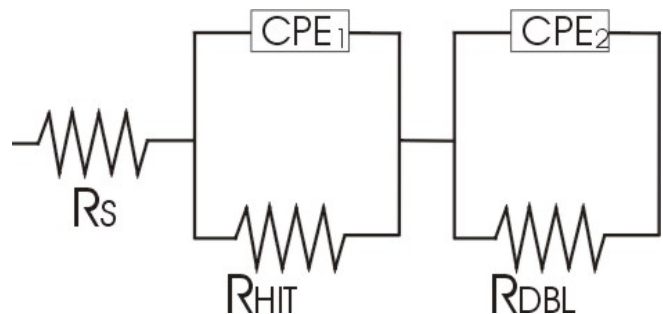


Figure 9. Typical equivalent electrical circuit for a conducting membrane; the CPE elements suggest a heterogeneous current flow on the membrane surface.

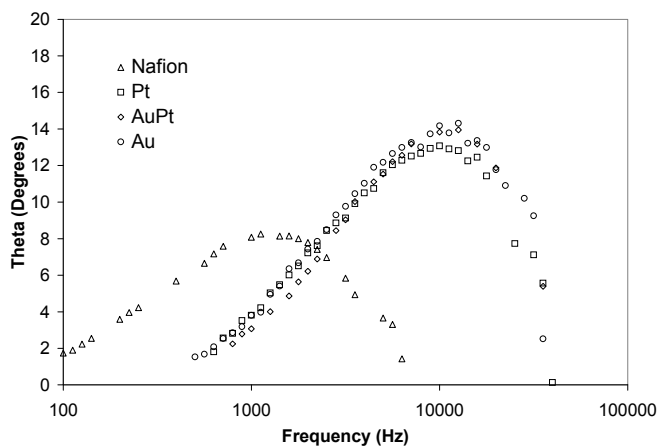


Figure 10. The Bode plots for the Nafion 115 and the self-assembled electrodes. For all the systems a main peak at a high frequency overlapped with a secondary peak at a low frequency can be observed.

ne/electrolyte interface is the determining step in the conduction process.

The membrane/electrolyte arrangement is considered as a heterogeneous system divided in two zones with different properties. In this way a two semicircle impedance response is expected (fig 8). The high frequency semicircle is related to the Heterogeneous Ionic Transfer (HIT) in the bulk membrane and a low frequency semicircle that represents the Diffusion Boundary Layer (DBL) in the membrane/electrolyte interface [31]. Another important characteristic of these systems is the semicircle depression due to the non-ideal behavior of the capacitive process. According to the results obtained by Jorcin et al [32] this response is typical for rough surfaces such as Nafion with a heterogeneous current flow and in this system the capacitors of the electrical equivalent circuits should be substituted by a Constant Phase Element.

Figure 10 shows the Bode plots (theta vs. Frequency). All the 4 membrane responses were similar, a high frequency well defined peak overlapped with a low frequency process. In the impregnated membranes the peak reaches a maximum at 10 kHz meanwhile in Nafion the higher theta value is located at 1 kHz. This peak displacement to the high frequency zone on impregnated membranes is related to the decrease of the Diffusion Boundary Layer Capacitance ( $C_{DBL}$ ) of the samples, as it can be seen in the  $C_{DBL}$  values of table 3.

When the power factor in the CPE is close to 1 ( $\eta \sim 1$ ), the  $Q_0$  value is directly proportional to the capacitance value, hence it is possible to say that the Nafion/Metal systems showed an important decrease in the boundary layer capacitance ( $C_{DBL}$ ). This decrease in the capacitance is closely related to the higher proton resistance ( $R_{HIT}$ ) observed in the self-assembled electrodes. It is easy to observe that the protonic charge accumulated in the Nafion surface is related to the capacitance in the membrane/electrolyte interface. The lower capacitance values for the impregnated membranes lead to a lower charge accumulation in the membrane channels close to the surface. According to the most recent proton conduction theory in Nafion [32], the protonic charge is transferred by forming and breaking hydrogen bonds in water wires confined in nanocavities in

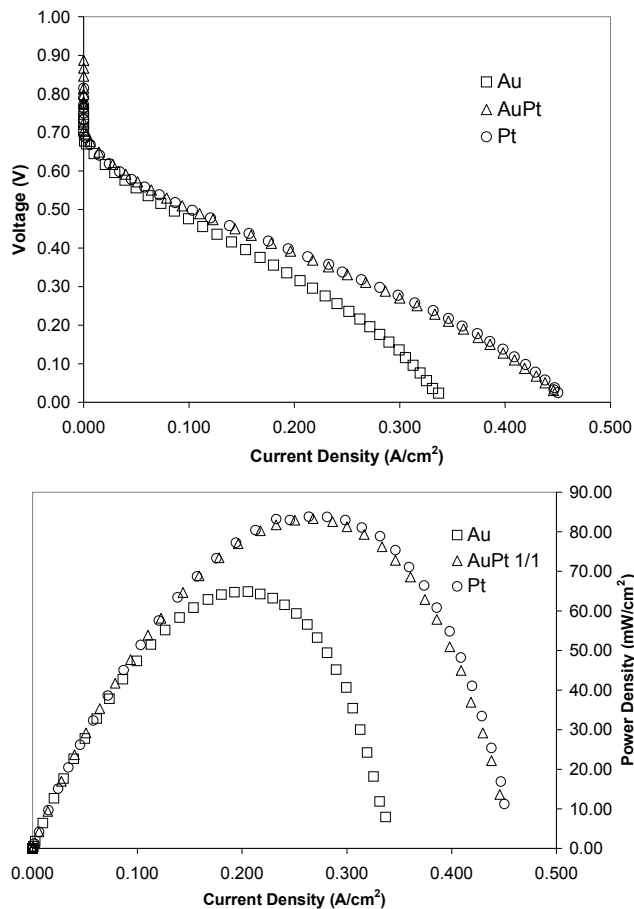


Figure 11. The polarization and power curves for the self-assembled electrodes.

the membrane channels. So, as expected the lack of protonic charge carriers in the self-assembled electrodes increases the proton conduction resistance as it can be seen in table 3.

### 3.5. Polarization Curve

The self-assembled electrodes fabricated with Nafion and catalytic nanoparticles were evaluated in a PEMFC load unit. The hydrogen and oxygen pressure was 1 atm with an anode flux of 100  $\text{cm}^3/\text{min}$  and cathode flux of 80  $\text{cm}^3/\text{min}$  and the temperature remained constant at 25°C. The MEAs fabricated with Nafion/Nanoparticles had an acceptable performance as seen in the polarization curves of figure 11. In all the MEAs the activation potential (potential at which the current starts increasing) was close to 0.7 V. When the current density increases the potential in the Nafion/Au self-assembled MEA drops faster than the Nafion/Pt and Nafion/AuPt MEAs because of its higher protonic resistance (table 4).

The self-assembled Nafion/AuPt had the best open circuit potential (887 mV) meanwhile the Au and Pt self-assemblies showed a similar performance in terms of maximum power and maximum current density. The Nafion/Au self-assembly performance was more affected by ohmic losses mainly in the membrane. The maximum power generation was obtained at 0.35 V, after this value the mass transport losses increase affecting the PEMFC efficiency.

#### 4. CONCLUSIONS

The Au-Pt nanoparticles were obtained by chemical reduction. The nanoparticle size in the three systems was close to 2 nm. Colloidal solutions were used to build self-assembled electrodes with nanoparticles deposited on Nafion membrane, a method for lowering the Pt content in the MEA. The particles deposited on Nafion had good stability and homogeneous distribution along the membrane surface. The particles deposited on Nafion showed a direct relation between the size and location with the hydrophilic and hydrophobic distribution phases of the membrane and its interaction with the nanoparticle synthesis elements.

The impedance results proved an increase in the membrane proton resistance of the self-assembled electrodes compared to unmodified Nafion. The increase in resistance is related to the diminution of the protonic charge carriers in the Nafion nanochannels near the surface due to the channel obstruction. Also, the impedance data analysis proved that the main membrane resistance is located between the membrane and the electrolyte and not in the bulk of the membrane, hence the main efforts in the conduction improvement should emphasize in lowering the energy barrier in the Diffusion Boundary Layer.

The self-assembled electrodes had a good performance at standard conditions. It is necessary to find the optimum colloidal concentration and immersion time in order to obtain good catalytic activity and high membrane conductance. The catalytic activity of the nanoparticles and the membrane resistance determine the I-V response of the self-assembled electrodes in the PEMFC evaluation.

#### 5. ACKNOWLEDGEMENTS

The authors acknowledge the grant received from CONACYT through the project CIAM 42146.

#### 6. REFERENCES

- [1] W. Smith, *Journal of Power Sources*; 86 (2000) 74.
- [2] T. Susai, A. Kawakami, A. Hamada, Y. Miyake, Y. Azegami, *Journal of Power Sources*; 92 (2000) 131.
- [3] E. Middelmann, W. Kout, B. Vogelaar, J. Lenssen, E. de Waal, *Journal of Power Sources*; 118 (2003) 44.
- [4] H. Chang, P. Koschany, C. Lim, J. Kim, *New Materials for Electrochemical Systems*, 3 (2000) 55.
- [5] D. Raistrick, in: R.E. White, K. Kinoshita, J.W. Van Zee, H.S. Burney, *Proc. Symposium on Diaphragms, Separators and Ion Exchange Membranes*; 86-13 (1986) 172.
- [6] S. Srinivasan, E.A. Ticianelli, C.R. Derouin, A. Redondo, *Journal of Power Sources*; 22 (1988) 359.
- [7] Wu-Hsun Cheng, Kao-Ching Wu, Man-Yin Lo, Chiou-Hwang Lee, *Catalysis Today*; 97 (2004) 145.
- [8] Mark A. Aubart, Bert D. Chandler, Rachael A. T. Could, Don A. Krogstad, Marcel F. J. Schoondergang, and Louis H. Pignolet, *Inorganic Chemistry*; 33 (1994) 3124.
- [9] Don A. Krogstad, Wayde V. Konze, and Louis H. Pignolet, *Inorganic Chemistry*; 35 (1996) 6763.
- [10] D. Gruber, N. Ponath, J. Müller and F. Lindstaedt, *Journal of Power Sources*; 150 (2005) 67.
- [11] M. Besson, A. Kallel, P. Gallezot, R. Zanella, C. Louis, *Catalysis Communications*; 4 (2003) 471.
- [12] M. Haruta, N. Yamada, T. Kobayashi, S. Iijima, *Journal of Catalysis*; 115 (1989) 301.
- [13] G.J. Hutchings, *Journal of Catalysis*; 96 (1985) 292.
- [14] A.M. Venezia, V. La Parola, V. Nicoli, G. Deganello, *Journal of Catalysis*; 212 (2002) 56.
- [15] Q. Fu, A. Weber, M. Flytzani-Stephanopoulos, *Catalysis Letter*; 77 (2001) 87.
- [16] J. Zhong, M.M. Maye, *Advanced Materials*; 13 (2001) 1507.
- [17] M.M. Maye, J. Luo, L. Han, N.L. Kariuki, C.-J. Zhong, *Gold Bulletin*; 36 (2003) 75.
- [18] C. J. Zhong, J. Luo, M.M. Maye, L. Han, N. Kariuki, *Proceeding of the GOLD 2003*, Vancouver, Canada, September–October (2003).
- [19] A.G. Hombrados, L. González, M.A. Rubio, W. Agila, E. Villanueva, D. Guinea, E. Chinarro, B. Moreno and J.R. Jurado, *Journal of Power Sources*; 151 (2005) 25.
- [20] Alex Hakenjos, Marco Zobel, Jan Clausnitzer and Christopher Hebling, *Journal of Power Sources*; 154 (2006) 360.
- [21] E. Bradley Easton and Peter G. Pickup, *Electrochimica Acta*; 50 (2005) 2469.
- [22] S. Slade, S.A. Campbell, T.R. Ralph, F.C. Walsh, *Journal of the Electrochemical Society*; 149 (2002) 1556.
- [23] V. Tricoli, N. Carretta, M. Bartolozzi, *Journal of the Electrochemical Society*; 147 (2000) 1286.
- [24] Jin Liu, Huanting Wang, Shaoan Cheng, Kwong-Yu Chan, *Journal of Membrane Science*; 246 (2005) 95.
- [25] Mohamed S. El-Deab, Takeo Ohsaka, *Electrochimica Acta*, 47, 4255, (2002).
- [26] Xianfeng Li, Chengji Zhao, Hui Lu, Zhe Wang, Hui Na, *Polymer*; 46 (2005) 5820.
- [27] Yu Seung Kim, Michael A. Hickner, Limin Dong, Bryan S. Pivovar, James E. McGrath, *Journal of Membrane Science*; 243 (2004) 317.
- [28] M. S. McGovern, E. C. Garnett, C. Rice, R. I. Masel and A. Wieckowski, *Journal of Power Sources*; 115 (2003) 35.
- [29] Shichun Mu, Haolin Tang, Zhaohui Wan, Mu Pan, Runzhang Yuan, *Electrochemistry Communications*; 7 (2005) 1143.
- [30] Yo Jin Kim, won Choon Choi, Seong Ihl Woo, Won Hi Hong, *Electrochimica Acta*; 49 (2004) 3227.
- [31] Jin-Soo Park, Jae-Hwan Choi, Kyeong-Ho Yeon, Seung-Hyeon Moon, *Journal of Colloid and Interface Science*; 294 (2006) 129.
- [32] Jean-Baptiste Jorcin, Mark E. Orazem, Nadine Pébère and Bernard Tribollet, *Electrochimica Acta*; 51 (2006) 1473.
- [33] Kreuer KD, *Journal of Membranes Science*; 185 (2001) 29.

